Multi-path charge transport in organic single crystals: a effective strategy to realizing ultra-sensitive organic ultraviolet photodetectors

Derui Zhu[1]†, Hongzhuo Wu[2]†, Zewei Li[1]†, Meyang Yu[1], Jingwei Tao[1]*, Lijun Zhang[1]*

[1] Key Laboratory of Automobile Materials of Ministry of Education and School of Materials Science and Engineering, Jilin University, Changchun, 130012, China

[2] Key Lab for Special Functional Materials of Ministry of Education, National and Local Joint Engineering Research Center for High-Efficiency Display and Lighting Technology, Collaborative Innovation Center of Nano Functional Materials and Applications, School of Nanoscience and Materials Engineering, Henan University, Kaifeng, 475004, China

†These authors contributed equally to this work.

*Corresponding author. E-mail: taojingwei@jlu.edu.cn, lijun_zhang@jlu.edu.cn

The temperature-dependent free-exciton emission intensities of 4,8-DTEBDT and 2,6-DTEBDT can be fitted using:

$$\mathrm{I}(T) = I_0/(1 + Ae^{-E_B/kT}) \quad \text{(S1)}$$

where I_0, E_B, and k is the intensity at 0 K, the binding energy, and the Boltzmann constant, respectively.

The field effect mobility (μ) of BDPEBD SC-OFETs was calculated in the saturation regime by the equation:

$$I_{DS} = WC_i\mu(V_G - V_{th})^2 / 2L \quad \text{(S2)}$$

where I_{DS}, W, and L are the drain current, the channel width, and the channel length, respectively. C_i is the capacitance of the insulation layer (300 nm SiO_2, 10 nF cm^{-2}), V_G is the gate voltage, and V_T is threshold voltage. All measurements were performed at room temperature in atmosphere.

The photosensitivity (P), photoresponsivity (R), detectivity (D^*), and external quantum efficiency (EQE) were calculated by the four equations:

$$P = \left|I_{photo} - I_{dark}\right| / I_{dark} \quad \text{(S3)}$$

$$R = \left|I_{photo} - I_{dark}\right| /(SP_i) \quad \text{(S4)}$$

$$D^* = S^{1/2}R/(2eI_{dark})^{1/2} \quad \text{(S5)}$$

$$EQE = \frac{(I_{photo}/I_{dark})hc}{eP_i\lambda_{peak}} \quad \text{(S6)}$$

where I_{photo} and I_{dark} are the drain-source current measured under illumination and the drain-source current measured in dark, P_i, S, h, c, e, and λ_{peak} are the incident light intensity, the area of illuminated channel, the Planck constant, the light velocity, the unit of charge, and the excitation wavelength, respectively.

Synthesis of compound 2

Compound 1 (2.594 g, 8 mmol), bis(triphenylphosphine)palladium(II) dichloride (0.280 g, 0.4 mmol), and copper(I) iodide (0.152 g, 0.8 mmol) were successively added to the sealed tube, and dissolved in 30 mL tetrahydrofuran and 30 mL diisopropylamine under nitrogen atmosphere, then trimethylsilylacetylene (0.982 g, 10 mmol) was added. The mixed solution

was stirred at 80 ℃ for 12 hours. The reaction mixture was filtered by the sand plate filter which the silica gel is added and washed by dichloromethane under vacuum, then concentrated under reduced pressure. The concentrated filtrate eluted through a silica gel column with petroleum ether to afford compound 2 as light yellow oil (2.59 g, 95%). ^{1}H NMR (500 MHz, CD_2Cl_2 δ): 7.34-7.30 (m, 6H), 7.14–7.11 (m, 6H), 6.96 (d, J = 8.0 Hz, 2H), 0.27 (s, 9H); MS (EI) m/z: 341.14.

Synthesis of compound 3

Compound 2 (2.05 g, 6 mmol) was dissolved in 50 mL dichloromethane, and then tetrabutylammonium fluoride (9 mL, 1 mol L^{-1} in THF) was added. The mixed solution was stirred at room temperature for 30 minutes, and then was poured into 100 mL water, and extracted with dichloromethane. The organic phase was dried with $MgSO_4$ and concentrated under reduced pressure. The concentrated filtrate eluted through a silica gel column with petroleum ether/dichloromethane (V/V = 10/1) to afford compound 3 as white powder (1.6 g, 99%). ^{1}H NMR (500 MHz, CD_2Cl_2 δ): 7.36 (d, *J* = 8.6 Hz, 2H), 7.34-7.31 (m, 4H), 7.15-7.11 (m, 6H), 6.99 (d, *J* = 8.5 Hz, 2H), 3.11 (s, 1H). MS (EI) m/z: 269.05.

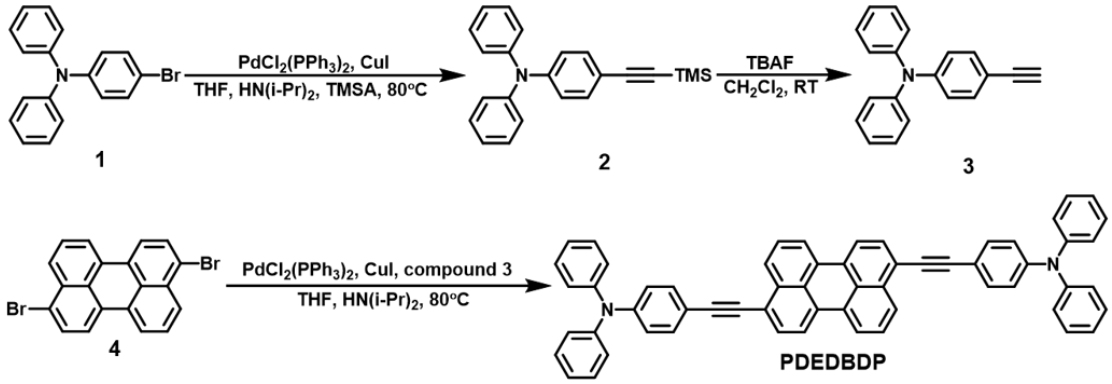

Supplementary Scheme 1 Synthetic route of PDEDBDP.

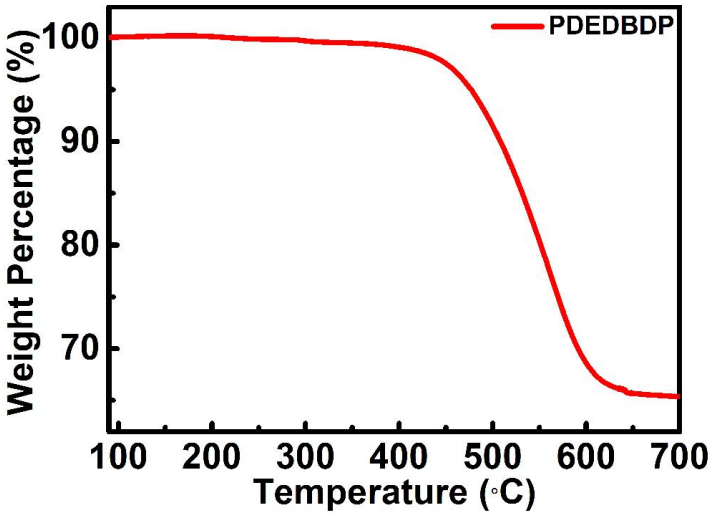

Supplementary Fig. 1 TGA of PDEDBDP.

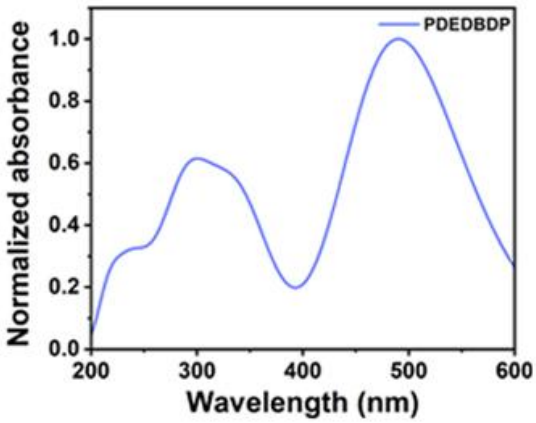

Supplementary Fig. 2 Normalized UV-vis spectra calculated by TDDFT: PDEDBDP.

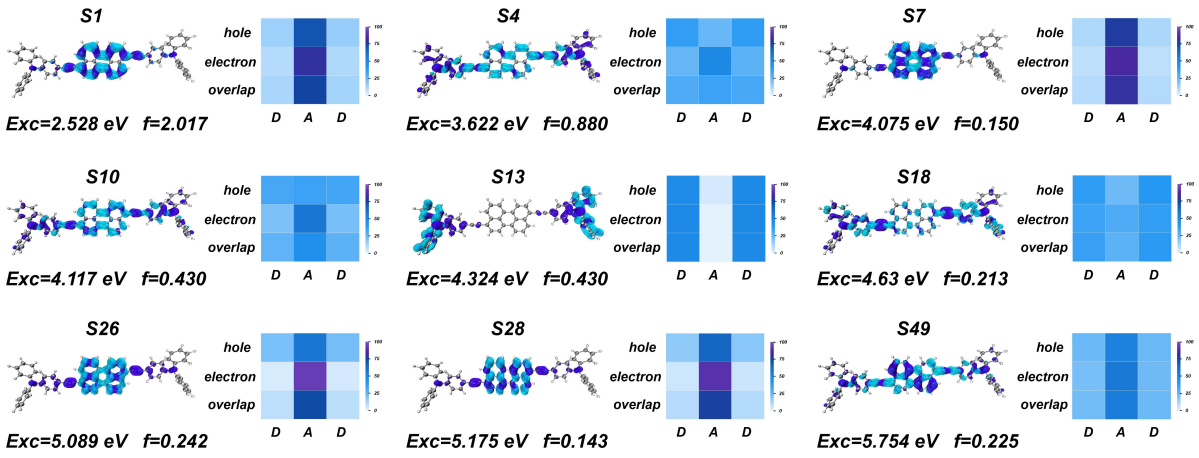

Supplementary Fig. 3 Distribution diagram of excited state wave functions, oscillator strength, and excitation energy for PDEDBDP.

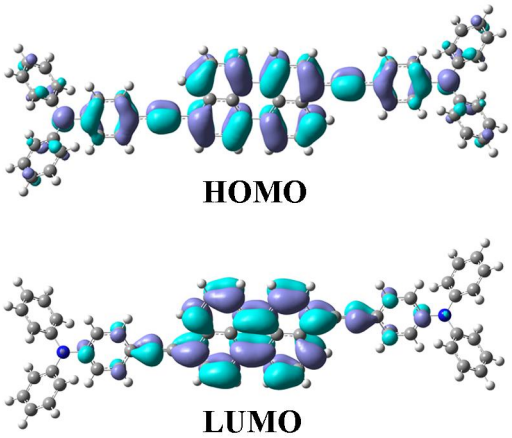

Supplementary Fig. 4 HOMO and LUMO orbitals of PDEDBDP calculated by DFT.

Supplementary Fig. 5 PDEDBDP single crystals.

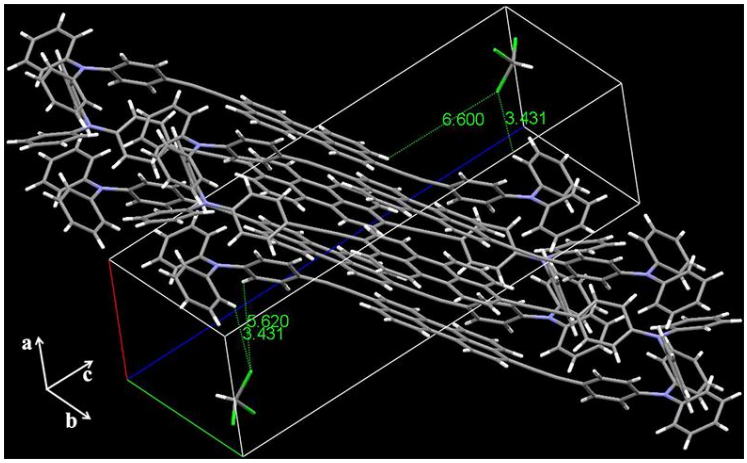

Supplementary Fig. 6 The single-crystal packing of PDEDBDP single crystal.

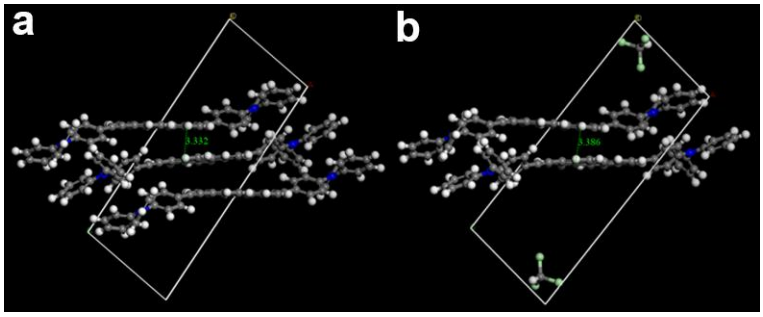

Supplementary Fig. 7 The CP2K combined with PBE0 and Auxiliary Density Matrix Methods (ADMM) to perform geometric relaxation on single crystal structures: A) eliminating chloroforml and B) containing chloroforml.

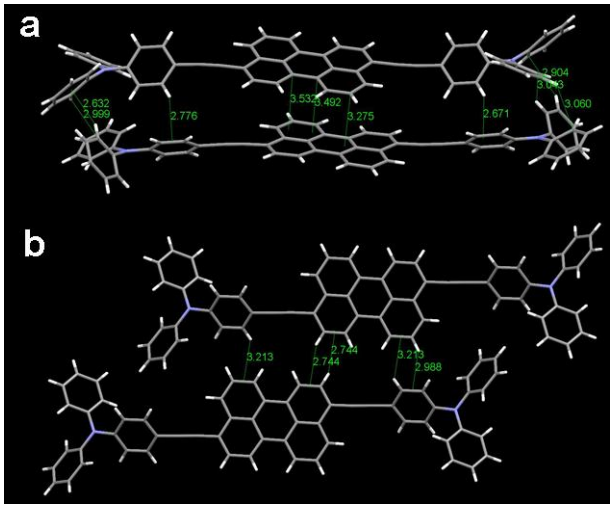

Supplementary Fig. 8 The intermolecular interaction in PDEDBDP single crystal.

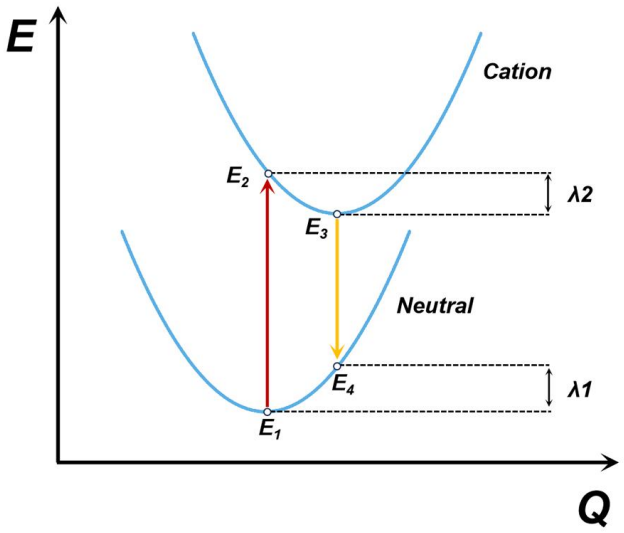

Supplementary Fig. 9 The reorganization energy is calculated via the four-point method, where λ1 and λ2 correspond to energy differences along the potential energy surfaces of the neutral and cationic states respectively. The plot displays energy (E) vertically versus geometric displacement (Q) horizontally.

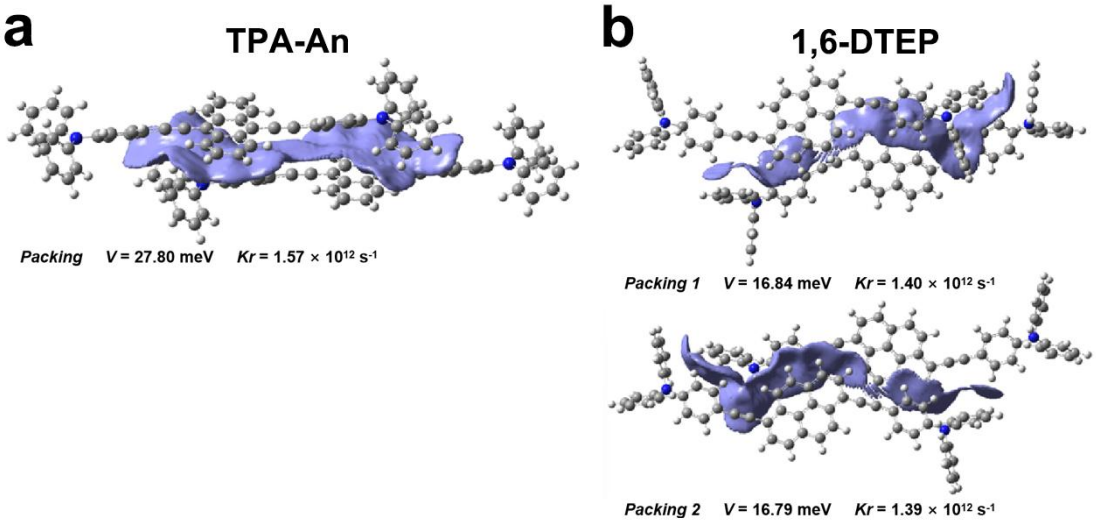

Supplementary Fig. 10 The intermolecular interactions calculated by IGMH in TPA-An (a) and 1,6-DTEP (b) single crystals.

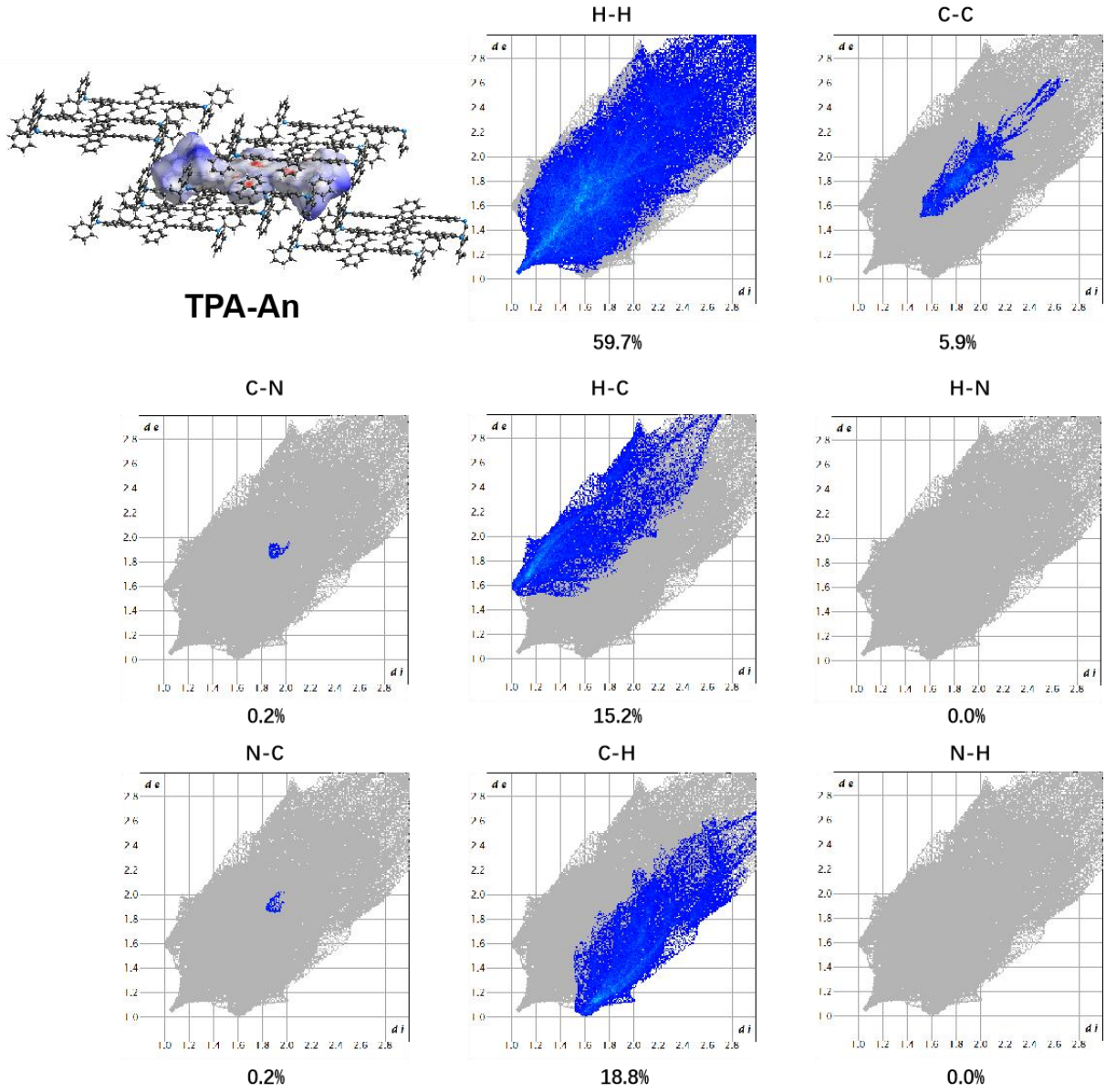

Supplementary Fig. 11 Hirshfeld surface analysis for the contribution of the interactions between different elements in TPA-An single crystal.

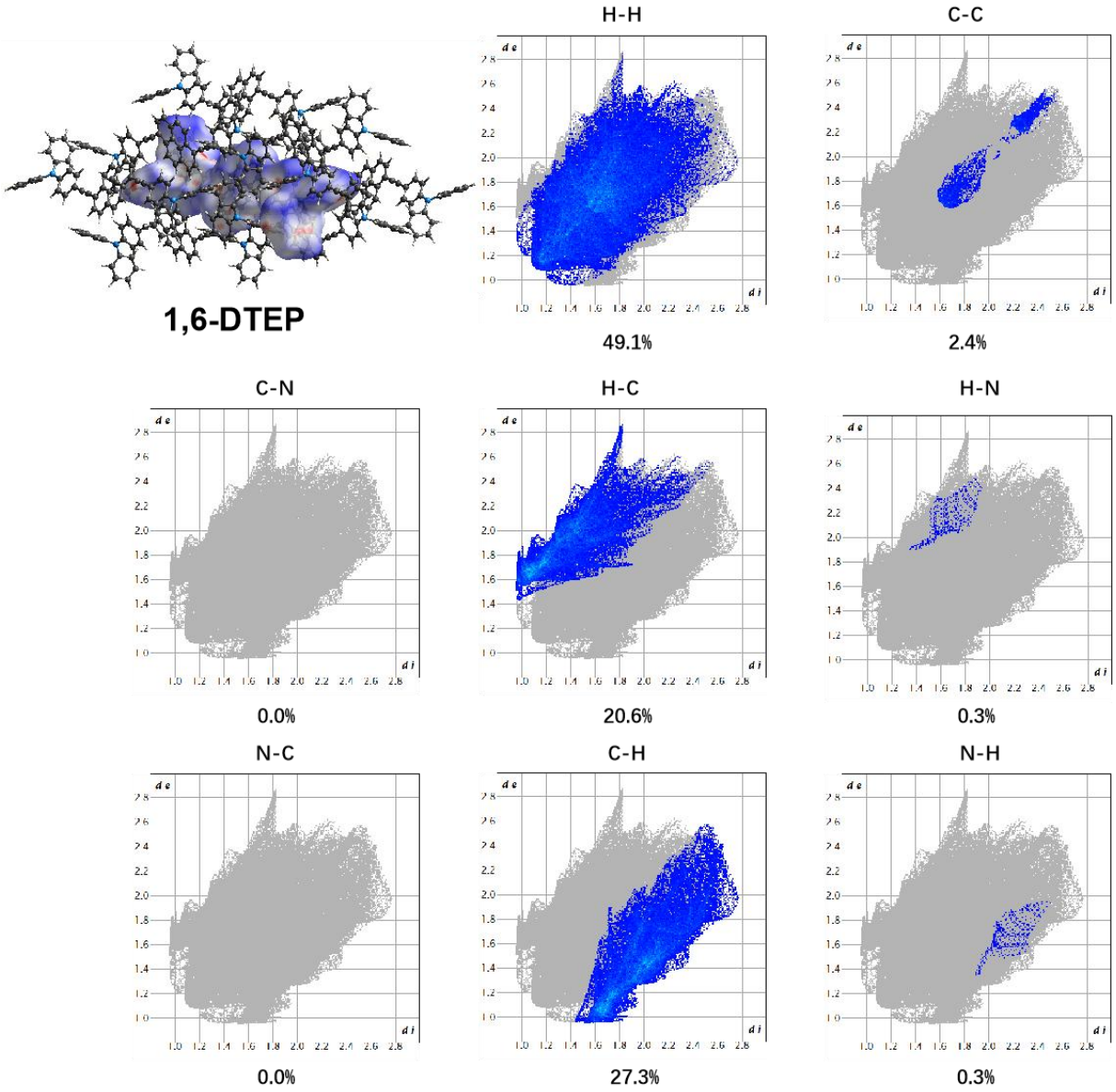

Supplementary Fig. 12 Hirshfeld surface analysis for the contribution of the interactions between different elements in 1,6-DTEP single crystal.

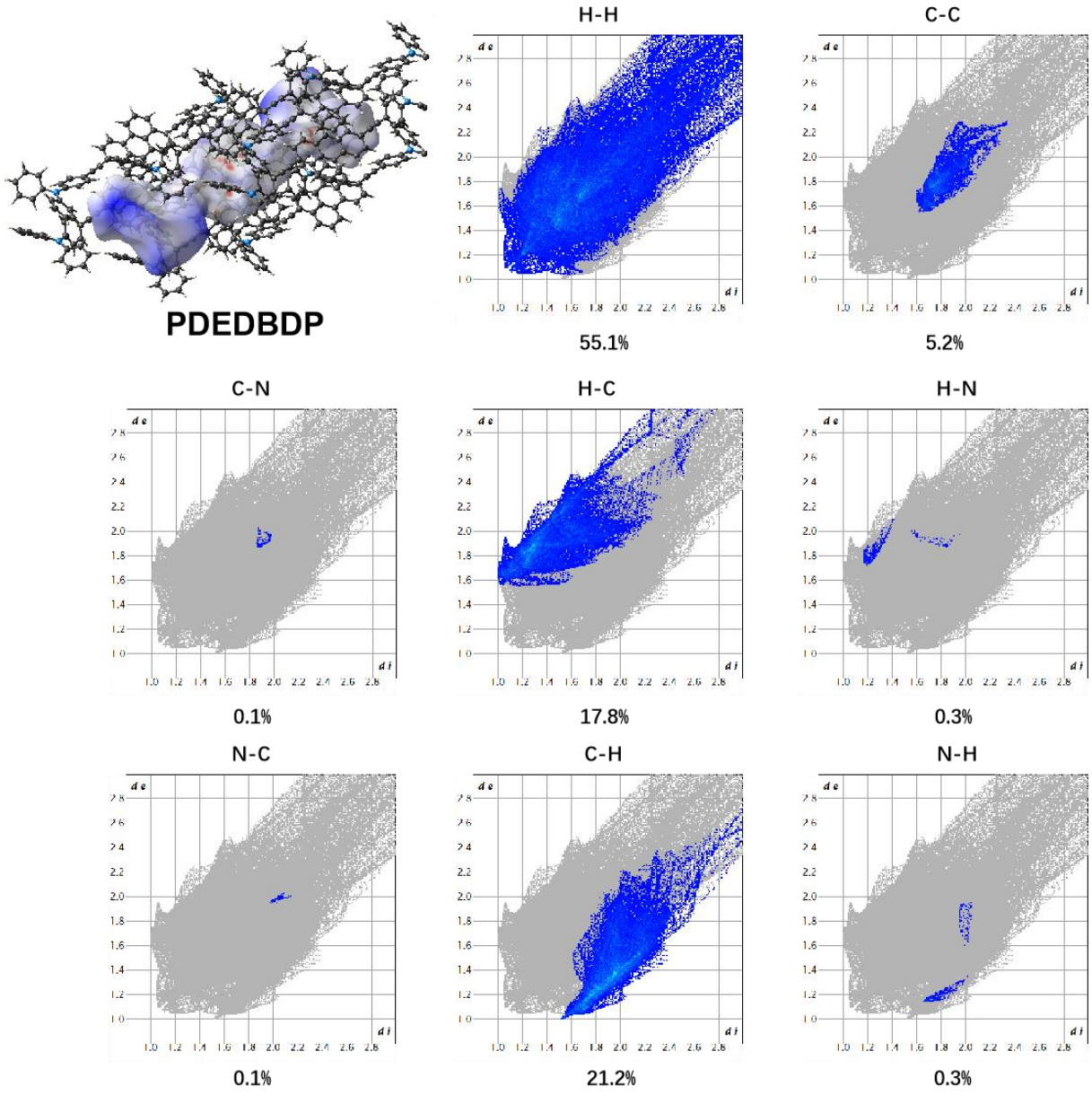

Supplementary Fig. 13 Hirshfeld surface analysis for the contribution of the interactions between different elements in PDEDBDP single crystal.

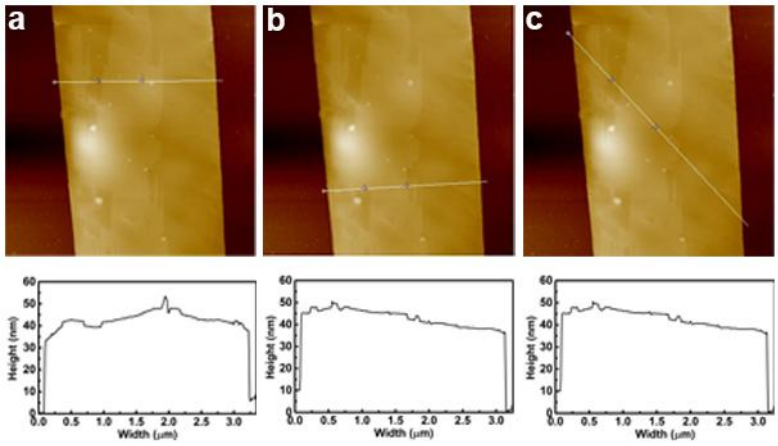

Supplementary Fig. 14 a, b, c, AFM images of the fabricated PDEDBDP SC-OFETs.

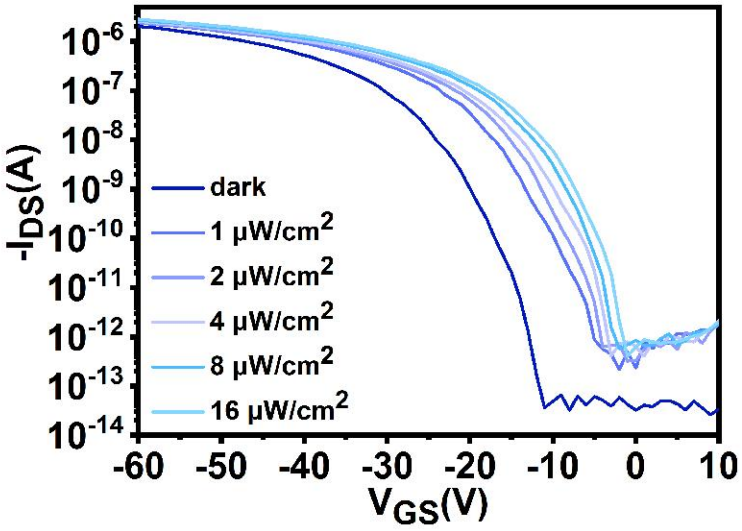

Supplementary Fig. S15 The transfer characteristics of PDEDBDP phototransistors in darkness and under various white light illumination intensities.

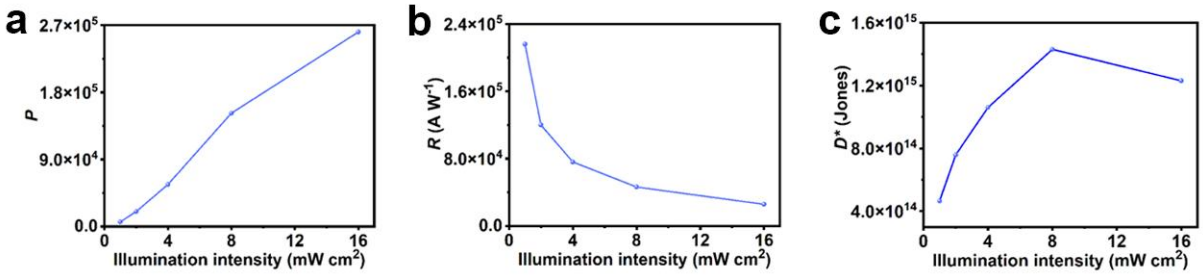

Supplementary Fig. 16 The dependence of P_{max}, R_{max}, and D^*_{max} (PDEDBDP device) under various white light illumination intensities.

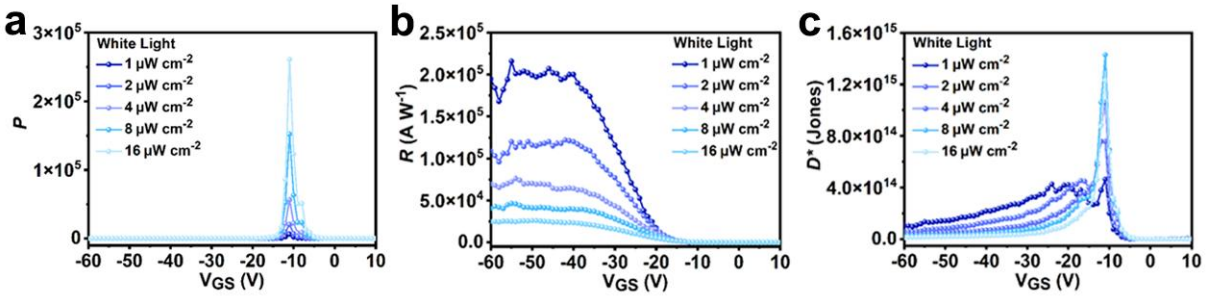

Supplementary Fig. 17 The effect of V_{GS} modulation on PDEDBDP device performance under various white light illumination intensities: P, R, and D^*.

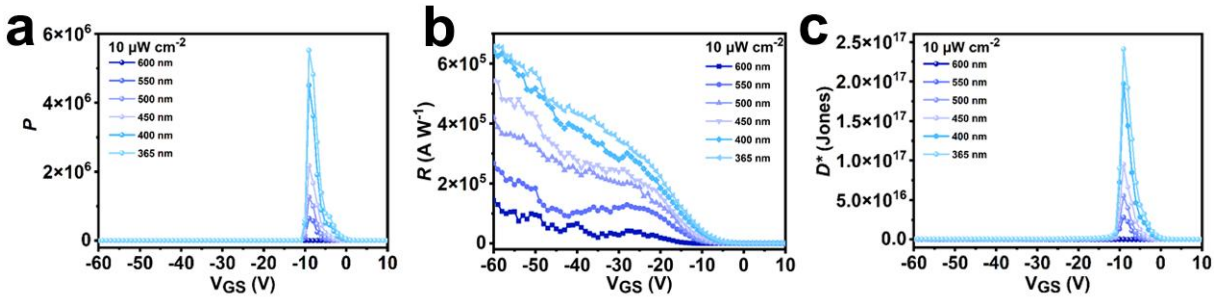

Supplementary Fig. 18 The effect of V_{GS} modulation on PDEDBDP device performance under 10 μW cm^{-2} different wavelength illumination: P, R, and D^*.

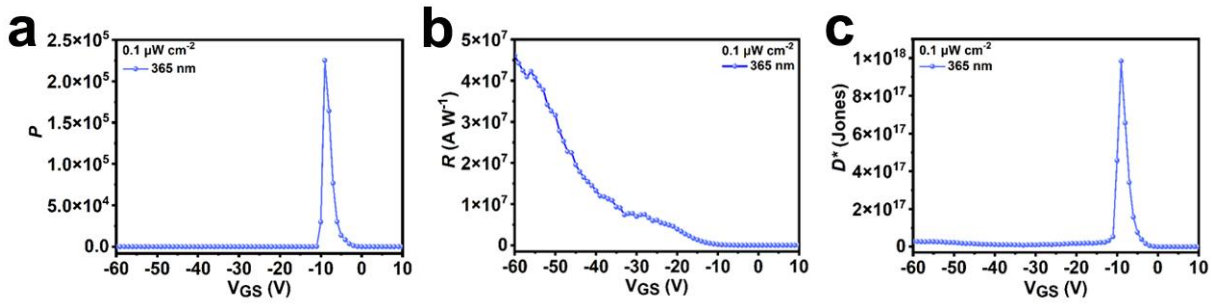

Supplementary Fig. 19 The effect of V_{GS} modulation on PDEDBDP device performance under 0.1 μW cm^{-2} different wavelength illumination: P, R, and D^*.

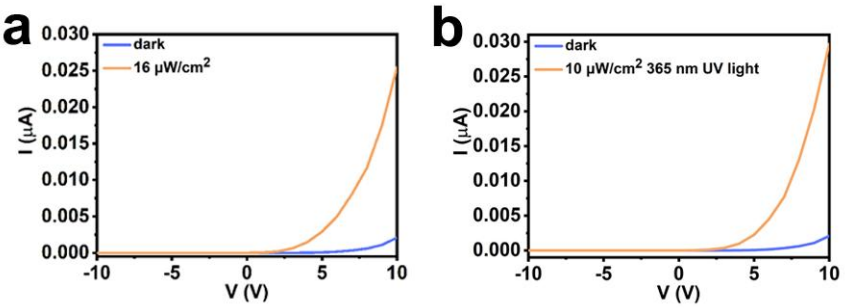

Supplementary Fig. 20 a, The *I-V* curves of photodiodes based on PDEDBDP micro/nanometersized single crystal in dark and under under 16 μW cm^{-2} white light illumination. **b,** The *I-V* curve of photodiodes based on PDEDBDP micro/nanometersized single crystal in dark and under under 10 μW cm^{-2} 365 nm light illumination.

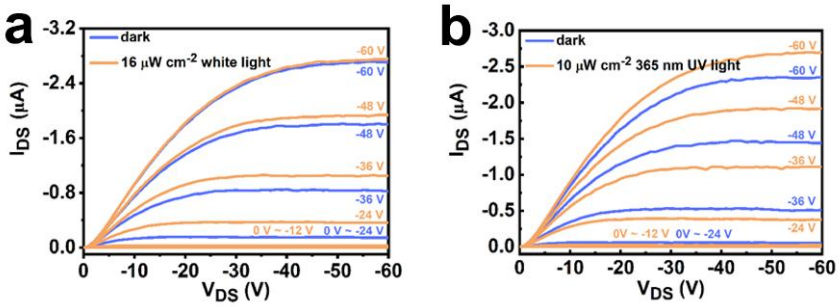

Supplementary Fig. 21 a, The output characteristics of the PDEDBDP SC-OPTs in darkness and under 16 μW cm^{-2} white light illumination. **b,** The output characteristics of the PDEDBDP SC-OPTs in darkness and under 10 μW cm^{-2} 365 nm UV light illumination.

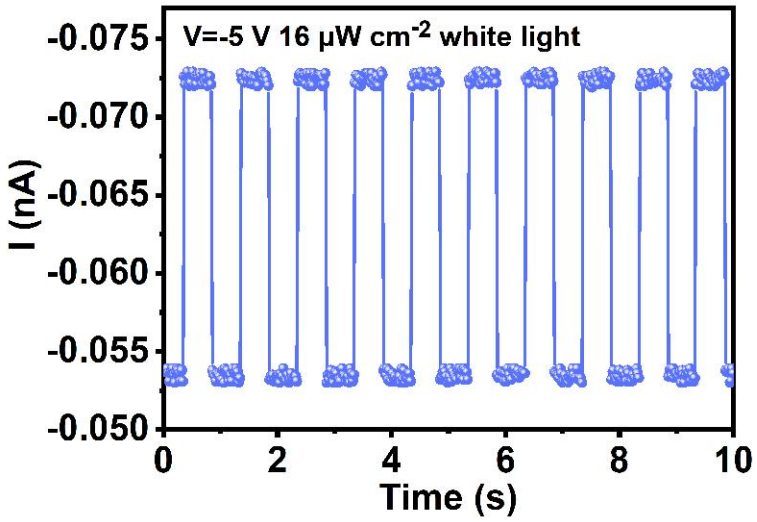

Supplementary Fig. 22 Temporal photoresponse of PDEDBDP device (ten cycles) under 16 μW cm^{-2} white light illumination.

Supplementary Table S1. HOMO levels, LUMO levels and optical bandgaps of PDEDBDP.

Compound	HOMO (eV)	LUMO (eV)	E_g^{opt} (eV)
PDEDBDP	-5.19	-3.07	2.12

Supplementary Table S2. The reorganization energy of TPA-An, 1,6-DTEP, and PDEDBDP single crystals.

Compound	E_λ (eV)
TPA-An	0.284
1,6-DTEP	0.208
PDEDBDP	0.213

Supplementary Table S3. PDEDBDP SC-OFET performances.

Compound	μ_{max} (μ_{avg}) [$cm^2\ V^{-1}\ s^{-1}$]	I_{on} / I_{off}	V_{Th} [V]
PDEDBDP	4.33 (1.53)	10^9～10^{10}	-2 ~ -10

Supplementary Table S4. PDEDBDP SC-OPT performances under various white light illumination intensities.

Compound	Light	P_i (μW cm^{-2})	P	R (A W^{-1})	D^* (Jones)
	white light	1	6.19×10^3	2.16×10^5	4.65×10^{14}
	white light	2	2.01×10^4	1.20×10^5	7.58×10^{14}
PDEDBDP	white light	4	5.64×10^4	7.61×10^4	1.06×10^{15}
	white light	8	1.52×10^5	4.64×10^4	1.43×10^{15}
	white light	16	2.61×10^5	2.59×10^4	1.23×10^{15}

Supplementary Table S5. PDEDBDP SC-OPT performances under 10 μW cm^{-2} different wavelength illumination.

Compound	Light	P_i (μW cm^{-2})	P	R (A W^{-1})	D^* (Jones)	EQE (%)
PDEDBDP	365 nm	10	5.52×10^6	6.58×10^5	2.41×10^{17}	1.54×10^8
	400 nm	10	4.51×10^6	6.41×10^5	1.97×10^{17}	1.13×10^8
	450 nm	10	2.17×10^6	5.44×10^5	9.49×10^{16}	5.73×10^7
	500 nm	10	1.26×10^6	4.21×10^5	5.50×10^{16}	2.94×10^7
	550 nm	10	6.41×10^5	2.68×10^5	2.80×10^{16}	1.52×10^7
	600 nm	10	3.08×10^5	1.43×10^5	1.40×10^{14}	1.45×10^5